Pathogenicity of three genetically distinct and highly pathogenic Egyptian H5N8 avian influenza viruses in chickens

Nahed Yehia (nahedyehia@gmail.com)
Animal health research institute https://orcid.org/0000-0002-2823-6467
Ahmed M Erfan
Animal Health Research Institute
amany adel
Animal Health Research Institute
marwa abdelmagid
Animal Health Research Institute
Wafaa M M Hassan
Animal Health Research Institute
Ahmed Samy
Animal Health Research Institute

Research Article

Keywords: Highly pathogenic avian influenza, Subtype H5N8, Clade 2.3.4.4b, Egypt, Chicken, Pathogenicity, Transmissibility.

Posted Date: April 2nd, 2021

DOI: https://doi.org/10.21203/rs.3.rs-372409/v1

Version of Record: A version of this preprint was published at Poultry Science on December 1st, 2021. See the published version at https://doi.org/10.1016/j.psj.2021.101662.

Abstract

In late 2016, Egypt was subjected to multiple introductions of reassorted highly pathogenic avian influenza viruses (HPAI) subtype H5N8. In a previous study, we reported three distinct genotypes during the first wave of infection represented by CAO285, SS19, and F446 viruses that were isolated from wild birds, backyard, and a commercial farm, respectively. F466 has subsequently become the predominant genotype currently circulating in Egypt and has been implicated in the emerging of the H5N2 virus. In the present study, we investigated the difference in the pathogenicity and transmissibility of the three genotypes. The intravenous pathogenicity index (IVPI) ranged from 2.68 to 2.9. With the natural route of infection, all these strains took longer to cause mortality in comparison to S75 (HPAI-H5N1). When compared the H5N8 viruses to each other showed that F446 had high mortality rate after inoculation from original concentration of 10^6 and 10^4 EID_{50} of virus. Chickens inoculated with F446 showed the highest viral titer with significant differnt in all tested samples (H5N8 and H5N1 viruses) in experimental and sentinel contact chicken with more efficient transmission to sentinel contact birds and spread from contact to other birds. Histopathological findings revealed the H5N1 and H5N8 viruses affect all organs examined (lung, trachea, brain, spleen) with relatively different affect the S75 cauterized by early marked respiratory adverse effect and F446 & SS19 were characterized by early systematic pathological alteration with mild respiratory pathological changes. The efficient viral replication and transmissibility in the main bird species, like chicken in case of Egypt, represent a key element for the spread and maintains of certain influenza genotypes of H5N8 virus and decrease the incidence of H5N1.

Introduction

Highly pathogenic avian influenza viruses (HPAI) caused by H5 subtype of type A influenza virus, family Orthomyxoviridae, first emerged in 1996 in the domestic goose in Guangdong (Gs/GD lineage) and has since been diagnosed in 80 countries causing huge economic losses. The zoonotic potential of this virus is also significant. Globally, from January 2003 to December 2020, in total 862 human infections have been reported for A(H5N1) with 455 fatalities and to date, 25 for A(H5N6) have been reported from China with eight cases proving fatal [1]. Gs/GD lineage viruses, unlike previous HPAI viruses, were isolated from wild birds [2] which may explain the rapid and global spread [3]. The Gs/GD lineage has evolved into 10 virus clades (0–9) with multiple subclades [4]. Among them, the group of viruses harboring the heamagglutinin gene (HA) of clade 2.3.4 acquired different neuraminidase genes, including N2, N5, and N8 via reassortment with other local avian influenza viruses. These viruses have been isolated from domestic birds in China, particularly in live poultry markets. Clade 2.3.4 has further evolved into 2.3.4.4 that includes the H5N2, H5N6, and H5N8 subtypes that have caused panzootic waves with severe losses to poultry production worldwide [5–7]. The HPAI-H5N8 clade 2.3.4.4 viruses were first detected in wild migratory waterfowl in China in 2013 [5] and genetic analysis has revealed two distinct genetic groups (A and B) were introduced into Korea in early 2014, likely via migratory birds [8, 9]. Group A was represented by A/broilerduck/Korea/Buan2/2014 while group B was represented by A/breeder duck/Korea/Gochang1/2014 [9]. In late 2014, group A spread to North America via long-distance migratory birds

where it reassorted with local LPAI viruses generating, among other viruses, H5N2 that became the predominant circulating virus in North America during 2014–2015 causing several outbreaks in poultry farms [10, 11]. Simultaneously, group A also spread westward to Europe and caused widespread outbreaks by the end of 2014 [12–14]. By mid-2016, a reassortant H5N8 HPAI Clade 2.3.4.4 group B, containing PB2, PB1 (polymerase basic 1,2), PA (polymerase acidic), NP (Nucleoprotein), and M (Matrix) segments from Eurasian LAPI, were detected in Qinghai Lake, China and Uvs-Nuur Lake in south Russia in dead wild birds [15, 16]. These novel viruses were further reassorted with Eurasian LPAI viruses which were disseminated over a huge geographical area in 2016, including Europe, Africa, Asia, and the Middle East along waterfowl migratory routes [9].

In Egypt, H5N8 HPAI Clade 2.3.4.4 group B was first reported late 2016 in wild birds on the north coast [17, 18]. From late 2016 to the present day, H5N8 has spread all over Egypt [19] and became the predominant HPAI-H5 virus in circulation, replacing the H5N1 viruses without any reported human cases [20]. Genetic analysis has revealed multiple introductions of reassortant H5N8 viruses [21, 22]. In late 2016 and early 2017, three distinguishable genotypes of H5N8 viruses have been reported [21], the first was represented by strain A/common-coot/Egypt/CA285/2016 (CA285) that was isolated from wild birds, the second was represented by A/duck/Egypt/SS19/2017 (SS19) that was isolated from backyard ducks and the third was represented by A/duck/Egypt/F446/2017 (F446) isolated from commercial duck farms. The F446 genotype became the predominant H5N8 circulating in Egypt containing PA and NP segments similar to A/mallard/Republic of Georgia/13/2011 (H6N2), while the remaining segments were more closely related to A/H5N8 viruses in wild birds from Uvs-Nuur Lake in south Russia (2016) [19]. The same reassortment pattern has been identified in Germany in many cases in wild birds in November 2016 [23]. Also, the F446 genotype possessess a higher potential for reassortment [24]. The predominance of the F446 like genotype does not exclude the possibility of other genotypes emerging and spreading in the future. Since to date the H5N8 viruses reassortment have occurred outside Egypt and viruses arrived with wild birds. The present study aims to elucidate the difference between pathogenicity and transmissibility between the three representative H5N8 genotypes in chickens. That might explain why F446 like strains become the predominant genotype.

Materials And Methods

Viruses:

A/common-coot/Egypt/CA285/2016 (H5N8) (CA285), A/duck/Egypt/SS19/2017 (H5N8) (SS19), and A/duck/Egypt/F446/2017 (H5N8) (F446) Viruses were isolated from swabs collected from wild birds, backyard, and a commercial farm respectively during the first wave of H5N8 spread in Egypt, viruses isolation, purification, and full genome sequencing were previously described [21] and A/chicken/Egypt/15S75/2015 (H5N1) (S75) used as a control. In the present study, all viruses were propagated by inoculation of diluted virus stock into the allantoic cavity of 11-day-old specific-pathogen-free embryonated chicken eggs (SPF-ECEs) and incubated at 37°C with daily candling, all embryos that died during the first 24hrs were excluded, the eggs were chilled for at least 4 hr at 4°C and then allantioc

fluid collected and the hemagglutination activity was tested [25]. Viruses were titrated in SPF-ECEs using egg infective dose 50% (EID50/ml) that was calculated by the Reed and Muench method [26].

Animal Experiments:

All animal experiments were conducted in negative pressure BSL3 isolators at the Reference Laboratory for Veterinary Control on Poultry Production (RLQP) of the Animal Health Research Institute (AHRI) and were approved by the scientific and biosafety committee of RLQP, AHRI, Egypt. All animal experiments were conducted following the recommendations and guidelines of the ministry of agriculture and land reclamation, Egypt.

Three experiments were conducted to examine the pathogenicity and replication pattern of the three H5N8 viruses and one H5N1 virus. In experiment 1, the intravenous pathogenicity index (IVPI) was measured following the reference procedure [25], briefly, ten 6-week-old SPF chickens (white leghorn) were inoculated with 0.1ml of each virus at > 4 log2 dilution, clinical signs scored daily for 10 days. Clinical signs include a respiratory manifestation, depression, diarrhea, cyanosis of the exposed skin or wattles, edema of the face, and/or head, nervous signs. Birds with none of these signs are considered as normal (scored 0), birds with one sign considered as sick (scored1) while birds with more than one of these signs are considered as severely sick (scored 2) and score 3 for dead birds. In Experiment 2, for each virus four dilutions (10^3 to 10^6 EID50/100µl) have been prepared, each dilution has been inoculated intranasal in five chickens of 4 weeks old. Chickens were observed for 10 days and any deaths were recorded two times per-day, birds with severe depression and about to die were humanely killed and counted as a deceased birds. Survival rates were statistically analyzed using the Kaplan–Meier method.

In experiment 3, 10^6 EID50/100 µl of each virus strain was inoculated into 10 SPF chickens and the next day three non-infected chickens of the same age were introduced to each group as sentinel contacts. Cloacal and tracheal swabs were collected from all birds at 2 and 4 days post-infection (dpi) for virus titration. Lung, spleen, and brain were collected aseptically from three infected birds from each group at 2 and 4 dpi or at death for virus titration and histopathological examination.

Quantifying the virus shedding and replication levels in different organs:

For viral titration, collected swabs and 0.1 g of collected organs were subjected to RNA extraction using QIAamp viral RNA mini kit (Qiagen, GmbH, Germany) following the manufacturer's instructions. Briefly, collected tissues were homogenized with an equal volume of PBS using the tissue lyser LT (Qiagen) and then subjected to three successive freeze-thaw cycles, then centrifuged at 12,000 g for 10 min to separate the supernatant. Swabs collected from each bird were placed individually in a viral transport medium. Individually pooled swabs were subjected to RNA extraction. RNA purity was measured by the NanoDropTM 2000 spectrophotometer (Thermo Scientific, Germany). The QuantiTect Probe RT-PCR kit (QIAGEN, Gmbh, Hilden, Germany) was used for reverse transcription and amplification of the H5 gene using specific primers and a TaqMan probe as previously described [27]. Each real-time RT-PCR run

included a ten-fold serial dilution of each strain tested to serve as a calibrator along with the no-template controls.

Statistical analysis

Data were coded and entered using the statistical package for the Social Sciences (SPSS) version 26 (IBM Corp., Armonk, NY, USA). Comparisons between groups were done using analysis of variance (ANOVA) with multiple comparisons post hoc test when comparing more than 2 groups [28]. Survival curves were plotted by the Kaplan-Meier method compared using the log-rank test [29]. P-values less than 0.05 were considered statistically significant.

Histopathological Evaluation:

We collected respiratory organs (Trachea and lung) and systemic organs (spleen) and nervous system organ (brain) for histopathology were immediately immersed in 10% neutral buffered formalin for fixation, paraffin-embedded, sectioned, and then stained with hematoxylin and eosin. Lesions were indexed following [30]. Slides representing each organ were prepared from three birds from each group at each time point.

Results

All the H5N8 strains used in the present study were isolated during the first wave of H5N8 in Egypt, where CAO258 recovered from wild birds in November 2016 [17], SS19 from backyard ducks in January 2017, and F446 from a commercial duck farm in April 2017 [21]. All belong to clade 2.3.4.4b, full genetic characterization revealed that they have high nucleotide similarity among HA, NA, M, and NS gene segments with the different origin of PB2, PB1, PA, and/or NP segment [21]. Further, S75 represents HPAI-H5N1 classic 2.2.1.2 isolated from commercial chicken farms in Egypt. Ten 6-week-old chickens were inoculated intravenously with 10^6 EID50 each of the four viruses. The IVPI was 2.73, 2.92, 2.78, and 2.68 for S75, CAO285, SS19 and F446 respectively. With 100% mortality at 2, 2, and 3 dpi for S75, CAO285 and SS19, whereas F446 induced 90% mortality at 4 dpi.

To investigate the survival rate using the natural route of infection, five chickens were intranasally inoculated with 10^3 to 10^6 EID50 of each strain and observed for ten days. The Kaplan-Meier survival curve with the calculation of median survival and unpaired log rank test were used in the survival between the groups. All chickens inoculated with 106EID50 of S75, SS19, F446 dead at 4 and 5 dpi. And, all chickens inoculated with 10^5 EID_{50} of S75 and F446, S/S19 died at 4, 9 and 10dpi, respectively. Whereas, 80% of birds died post-inoculation with 10^5 EID50 of CAO285 at 9dpi. With one log10 lower (10^4 EID50), 80 % of birds dead at 7 with strains S75 and 60% dead with strain F446 and SS19 at 9 dpi while CAO258 was fatal in 40% of birds at 9 dpi (Fig. 1). In addition, 80% of chicken dead after 6 dpi with 10^3 EID50 S75, 60% of chicken dead at 7-10dpi with 10^3 EID50 F446, S/S19 and CA285 (Fig. 1). The significance different (p-value)between all groups in all survival curves were less than 0.05 (Fig. 2).

To correlate between shedding and viral replication in different organs and viral pathogenicity, swabs, lung, spleen, and brain samples were collected at 2 and 4 dpi with 10^6 EID50 of each virus. Higher viral titers with significant differences were seen in all tested samples infected with strain F446 compared to strain CAO285 and SS19, correlating with significantly more transmission to the sentinel co-housed birds(Fig. 3, 4) (Table.1.) Further, strain F446 infected birds showed higher viral titers with significant differences in spleen and swabs in 2nd day comparing to S75 infected birds at 2 and 4 dpi. Also, in lung and brain in 4dpi only(Fig. 3, 4) (Table.1).The F446 was more efficiently transmitted to sentinel co-housed birds comparing to SS19 and CAO285 at 2 and 4 dpi and S75 at 2dpi.Two out of the three contact birds dead at 4 and 5 dpi with S75. And one contact bird at 6 dpi with F446 and SS19 with high viral titer with significant differences in F446 comparing with, SS19 and CAO285 in 2-4dpi andS75 in 2dpi. (Fig. 5) (Table.1).

Histopathological Results

Microscopic examination of the control group revealed the normal histological architecture of examined organs (Fig. 6). On the other hand, different pathological alterations were recorded in examined organs from infected groups.

Microscopically, the trachea of F446 showed submucosal edema and congested blood vessels 2dpi (Fig. 7a). Subsequently, a severe pathological alteration was recorded exhibited by hyperplasia of the mucous gland with luminal and submucosal inflammatory cells infiltration 4dpi (Fig. 8a). Meanwhile, the trachea of SS19 appeared with intact mucosa with submucosal hemorrhages and edema 2dpi (Fig. 7b) then revealed activation of mucous gland associated with luminal lymphocytic cells infiltration 4dpi (Fig. 8b). On the other hand, the trachea of CA258 showed early activation of the mucous gland with marked submucosal edema with congested blood vessels 2dpi (Fig. 7c) progressed to necrosed mucosal layer with lymphocytic cells infiltration 4dpi (Fig. 8c). On the contrary, the trachea of chicken infected with H5N1 S75 revealed severe tracheitis 2dpi exhibited by marked necrosed mucosal layer associated with lymphocytic cells infiltration and submucosal edema (Fig. 7d) while 4dpi showed activation of the mucous gland with lymphocytic cells infiltration (Fig. 8d).

The lung of F446 revealed prominent interstitial hemorrhages with congested pulmonary blood vessels and necrosis of 3ry bronchi epithelium associated with intraluminal inflammatory exudates 2dpi (Fig. 7e). On 4dpi, lung showed severe pneumonia appeared as massive hemorrhages within the parenchyma and thickening of alveolar with compensatory alveoli formation as well as massive inflammatory cells infiltration (Fig. 8e); lung of SS19 showed pulmonary hemorrhages with thickening blood vessel at 2dpi (Fig. 7f); progressed to vasculitis of pulmonary blood vessels 4dpc with massive lymphocytic cells infiltration inside the pulmonary blood vessels and within the parenchyma (Fig. 8f). On the other hand, lung of CA258 revealed acute picture 2dpi which showed marked vasculitis and thrombus formation with perivascular infiltration of lymphocytic cells (Fig. 7g); while 4dpi, the lung showed an area of necrosis (Fig. 8g). In the case of S75, the lung showed severe pneumonia exhibited by massive inflammatory cell

infiltration within the parenchyma and inside blood vessels associated with pulmonary hemorrhages 2dpi (Fig. 7h); also, marked vasculitis detected with fibrous tissue proliferation 4dpi (Fig. 8h).

Related to the spleen, the specimen of F446 and SS19 respectively showed lymphocytic depletion and necrosis associated with arteriosclerosis 2dpi (Fig. 7i&7j) which increased in severity with heterophils infiltration 4dpi (Fig. 8i&j). Meanwhile, CA258 showed normal histologic picture 2dpi (Fig. 7k) progressed to splenitis 4dpi (Fig. 8k) with heterophils infiltration and arteriosclerosis associated with mild lymphocytic depletion. Otherwise, the spleen of S75 showed the same picture of (CA258) (Fig. 7l &8l).

Regarding the brain, F446 revealed slight cerebral edema associated with congested blood vessels and hemorrhage 2dpi (Fig. 7m) which progressed to localized lymphocytic cells infiltration and neuronal necrosis 4dpi (Fig. 8m). Brian of SS19 showed multiple congested blood vessels and neuronal necrosis 2dpci (Fig. 7n) which increased in the severity 4dpc (Fig. 8n). In case of CA258, brain revealed cerebral edema and gliosis 2dpi (Fig. 7o) which increased 4dpi (Fig. 8o). Contrary, brain of S75 revealed congested cerebral blood vessels with diffuse neuronal necrosis 2dpc (Fig. 7p) which increased 4dpi (Fig. 8p)

Discussion

Since May/June 2016, HPAI-H5N8 clade 2.3.4.4b has caused panzootic waves across Asia, Europe, the Middle East, and Africa [31, 32]. In Egypt, the virus was first detected in wild birds in northern Egypt in late 2016 [17], since then it has spread all over Egypt and has been isolated from several different poultry production sectors causing massive economic losses [19]. A few months after the introduction of the virus to Egypt, a genotyping study revealed a multiple incursion pattern of HPAI-H5N8 viruses into Egypt [21] The first genotypes were recovered from wild birds in November 2016 (CAO285), followed by backyard ducks in January 2017 (SS19) and commercial duck farms in April 2017 (F446). All three of these genotypes showed high nucleotide similarity at the level of HA, NA, M, and NS gene segments close to 2.3.4.4b Russia–Mongolia 2016 reassortant isolates (eg., A/great crested grebe/Uvs-Nuur Lake/341/2016 (H5N8)), with PB2, PB1, PA and/or NP segments originated from different influenza viruses circulated in Asia and Europe [21]. Here, we investigated the difference in the pathogenicity and transmissibility of these three viruses in chickens that may help explain the current predominance of the F446-like strains [19] and its higher potential for reassortment [24]. To this end, IVPI, lethality, virus shedding, and dissemination in different organs, transmissibility as well as micro-pathogenicity were investigated in chickens infected with viruses representing these different genotypes.

We found that all tested strains were HPAI with IVPI ranging from 2.68 to 2.9 which corresponds with HA gene sequencing confirming the presence of multiple basic amino acid motifs PLREKRRKR/GLF at the cleavage site [21]. However, F446 caused 90 % mortality at 4 dpi comparing to 100% mortality at 2 and 3 dpi with CAO285 and SS19, respectively, which was closer to S75 (HPAI-H5N1) that also caused 100% mortality 2 dpi. In contrast, mortality was delayed with intranasally inoculation compared to S75 strains, with comparable results for CAO285 and F446 with a high dose of infection. In addition, marked lower

mortality in naive contact birds were observed for H5N8 inoculated genotypes. The intravenous inoculation of influenza viruses in chickens allows direct exposure of different organs beyond the natural route of infection [33], which can explain the comparable results of IVPI findings. While the intranasal inoculation represents the natural route of infection with delayed onset of mortality and lower transmissibility comparing to HPAI-H5N1. The same difference between comparing to HPAI-H5N1 has been reported for Korean and Japanese H5N8 viruses [34, 35]. Also, high mortality reaches 100%, 80% were recorded compared to other H5N8 viruses with intranasal inoculation of 10^6, and 10^5. F446 respectively reveal to high pathogenicity effect of F446 that was widely distributed recently in Egypt.

Higher viral titers with a significant difference were recovered from swabs, lung, spleen, and brains collected from chickens inoculated with F446 at 2 and 4 dpi compared with other H5N8 viruses in this study and also higher viral titer with significant differences in swabs at 2 dpi from contact chicken infected with F446 than other H5N8 viruses in this study. It indicates the higher transmissibility of F446 to the sentinel contact birds and higher spread from contact to other birds. The outperformance of the F446 strain compared to the other tested H5N8 strains in chickens may explain previous findings showing that F446-like reassortant strain is the predominant H5N8 strain in Egypt [19, 36, 37, 38]. And by the presence of multiple strains of avian influenza H5N1, H5N8 and H9N2 [37, 38] has predict many future recombinations as recorded in the novel reassortant H5N2 that showed 98–99% similarity with F446 suggesting that F446 is the donor virus and N2 from Egyptian H9N2 [24]. Also, F446 exhibited higher viral titer with significant differences comparing to S75 in the brain at 2, 4dpi and swabs at 2dpi, spleen and lung at 4dpi. It may explain the increased incidence of H5N8 than H5N1in 2017–2019 [37, 38].

Histopathological findings of H5N1 (S75) indicated that, respiratory organs are the primary target for influenza virus and also the choreographers for cytokines amplification during infection [39] that's responsible for the pathological alterations and pathogenesis of the disease in severe influenza infection; which quite similar to the picture of H5N8 (CA258) strain while other examined H5N8 strains (F446 & SS19) were characterized by early systematic pathological alteration more than respiratory adverse effect. Moreover, the F446 strain revealed more pathological alterations than the SS19 effect which correlated with virus titer in the same examined organs. The excessive immune response associated with H5N1 can worsen its pathogenesis and alters the viral replication in different organs, such a pathogenic state has been confirmed in different studies [40, 41]. Whether the H5N8 strains follow the same immunopathogenesis as HPAI-H5N1 with a different degree remains to be elucidated in future studies

the unadapted influenza polymerase complex leads to the generation of defective interfering influenzas viral RNA and unfunctional viral RNA that induces IFN activation and enhances the innate immune response. In contrast, a more 'adapted' influenza polymerase complex induces lower IFN expression that allows a more prolonged infection and viral shedding leading to increased viral transmission [42]. In light of these previous findings, it could be proposed for the efficient replication, comparable pathogenicity and predominance of the F446 like strain; 1st, early adaptation by serial passage in commercial ducks where it can silently spread with efficient transmission to other bird, 2nd the more adapted unique polymerase complex is due to the different origin NP and PA genes. Both scenarios require future researches based

on directed surveillance of ducks in backyard and commercial farms, as well as studying the impact of different polymerase reassortment by reverse genetic approaches.

Conclusions

Altogether, our data suggest that the predominance of F446-like strains in Egypt could be attributed to the relatively efficient replication and transmissibility in chicken due its high viral titer in swabs and organs other than H5N8 viruses and H5N1 virus, and these explain recently why the H5N1 were decrease and H5N8 had high incidence rate.

Declarations

Author Contributions: Author Contributions: Conceptualization, A.S. animal experiments N.Y. Histopathology M.A.; N.Y.; methodology, A.M.E.; A. A validation, N.Y.; A.M.E., and W.M.H.; Data curation, A.S., A.M.E., and N.Y Writing original draft, A.S.; writing review and editing, A.M.E, MA and A.S.; All authors have read and agreed to the published version of the manuscript.

Funding: all animal experiments supported by the core fund of the Reference Laboratory for Quality Control on Poultry Production, Animal Health Research Institute, Agriculture Research Center, Egypt.

Acknowledgments: The authors would like to thank colleagues in animal experimental facilities in RLQP for their technical help. Also, we would like to thank prof. John Hammond and Dr. Andreas Alber from Pirbright institute for their valuable comments on the manuscript. We would like to thanks prof Dr. Kawkab Abdelaziz for her support. Ahmed Samy is currently supported by the Bill and Melinda Gates Foundation [108704-001] and BBS/E/I/00007038.

Conflicts of Interest: The authors declare no conflict of interest.

References

1. WHO, Human infection with avian influenza A(H5) viruses. Available at <https://www.who.int/docs/default-source/wpro—documents/emergency/surveillance/avian-influenza/ai-20200424.pdf?sfvrsn=223ca73f_48> Accessed 24 April 2020.
2. Rohm, C., et al., Do hemagglutinin genes of highly pathogenic avian influenza viruses constitute unique phylogenetic lineages? Virology, 1995. 209(2): P. 664-70.
3. Swayne, D., et al. Impact of emergence of avian influenza in North America and preventative measures. in Proceedings of the Sixty-Fifth Western Poultry Disease Conference. 2016.
4. , OIE., and FAO., Toward a unified nomenclature system for highly pathogenic avian influenza virus (H5N1). Emerging infectious diseases, H5N1 Evolution Working Group 2008. 14(7): P. e1-e1.
5. Gu, M., et al., Novel reassortant highly pathogenic avian influenza (H5N5) viruses in domestic ducks, China. Emerging infectious diseases, 2011. 17(6): P. 1060-1063.

6. Wu, H., et al., Novel reassortant influenza A(H5N8) viruses in domestic ducks, eastern China. Emerging infectious diseases, 2014. 20(8): P. 1315-1318.
7. Zhao, G., et al., Novel Reassortant Highly Pathogenic H5N2 Avian Influenza Viruses in Poultry in China. PLoS ONE, 2012. 7(9): P. e46183.
8. Jeong, J., et al., Highly pathogenic avian influenza virus (H5N8) in domestic poultry and its relationship with migratory birds in South Korea during 2014. Vet Microbiol, 2014. 173(3-4): P. 249-57.
9. Lee, D.H., et al., Evolution, global spread, and pathogenicity of highly pathogenic avian influenza H5Nx clade 2.3.4.4. J Vet Sci, 2017. 18(S1): P. 269-280.
10. Pasick, J., et al., Reassortant Highly Pathogenic Influenza A H5N2 Virus Containing Gene Segments Related to Eurasian H5N8 in British Columbia, Canada, 2014. Scientific Reports, 2015. 5(1): P. 9484.
11. Lee, D.H., et al., Highly Pathogenic Avian Influenza Viruses and Generation of Novel Reassortants, United States, 2014-2015. Emerg Infect Dis, 2016. 22(7): P. 1283-5.
12. Harder, T., et al., Influenza A(H5N8) Virus Similar to Strain in Korea Causing Highly Pathogenic Avian Influenza in Germany. Emerg Infect Dis, 2015. 21(5): P. 860-3.
13. Hanna, A., et al., Genetic Characterization of Highly Pathogenic Avian Influenza (H5N8) Virus from Domestic Ducks, England, November 2014. Emerg Infect Dis, 2015. 21(5): P. 879-82.
14. Bouwstra, R.J., et al., Phylogenetic analysis of highly pathogenic avian influenza A(H5N8) virus outbreak strains provides evidence for four separate introductions and one between-poultry farm transmission in the Netherlands, November 2014. Euro Surveill, 2015. 20(26).
15. Li, M., et al., Highly Pathogenic Avian Influenza A(H5N8) Virus in Wild Migratory Birds, Qinghai Lake, China. Emerging infectious diseases, 2017. 23(4): P. 637-641.
16. Lee, D.H., et al., Novel Reassortant Clade 2.3.4.4 Avian Influenza A(H5N8) Virus in Wild Aquatic Birds, Russia, 2016. Emerg Infect Dis, 2017. 23(2): P. 359-360.
17. Selim, A.A., et al., Highly Pathogenic Avian Influenza Virus (H5N8) Clade 2.3.4.4 Infection in Migratory Birds, Egypt. Emerg Infect Dis, 2017. 23(6): P. 1048-1051.
18. Kandeil, A., et al., Genetic characterization of highly pathogenic avian influenza A H5N8 viruses isolated from wild birds in Egypt. J Gen Virol, 2017. 98(7): P. 1573-1586.
19. Yehia, N., et al., Genetic variability of avian influenza virus subtype H5N8 in Egypt in 2017 and 2018. Arch Virol, 2020.
20. El-Shesheny, R., et al., H5 Influenza Viruses in Egypt. Cold Spring Harb Perspect Med, 2020.
21. Yehia, N., et al., Multiple introductions of reassorted highly pathogenic avian influenza viruses (H5N8) clade 2.3.4.4b causing outbreaks in wild birds and poultry in Egypt. Infect Genet Evol, 2018. 58: P. 56-65.
22. Salaheldin, A.H., et al., Multiple Introductions of Influenza A(H5N8) Virus into Poultry, Egypt, 2017. Emerging infectious diseases, 2018. 24(5): P. 943-946.

23. Pohlmann, A., et al., Outbreaks among Wild Birds and Domestic Poultry Caused by Reassorted Influenza A(H5N8) Clade 2.3.4.4 Viruses, Germany, 2016. Emerg Infect Dis, 2017. 23(4): P. 633-636.
24. Hagag, N.M., et al., Isolation of a Novel Reassortant Highly Pathogenic Avian Influenza (H5N2) Virus in Egypt. Viruses, 2019. 11(6).
25. , World Organisation for Animal Health (OIE) Terrestrial Manual 2018. Chapter 3.3.4. Avian Influenza —Infection with Avian Influenza Viruses. 821–843. Available online: https://www.oie.int/fileadmin/Home/eng/Health_standards/tahm/3.03.04_AI.pdf (accessed on 11 March 2019). 2018.
26. REED, L.J. and H. MUENCH, A SIMPLE METHOD OF ESTIMATING FIFTY PER CENT ENDPOINTS12. American Journal of Epidemiology $V 27, 1938(3): P. 493-497.
27. Löndt, B.Z., et al., Pathogenesis of highly pathogenic avian influenza A/turkey/Turkey/1/2005 H5N1 in Pekin ducks (Anas platyrhynchos) infected experimentally. Avian Pathol, 2008. 37(6): P. 619-27.
28. Chan YH (2003): Biostatistics102: Quantitative Data – Parametric & Non-parametric Tests. Singapore Med J.;44(8): 391-396.
29. Chan YH (2004): Biostatistics 203: Survival analysis. Singapore Med J,;45(6) : 249
30. Survana, K.S.L., Ch, and Bancroft. (2013).Theory and practice of histological techniques. 7th ed., Churchill, Livingston: New York.
31. Kleyheeg, E., et al., Deaths among Wild Birds during Highly Pathogenic Avian Influenza A(H5N8) Virus Outbreak, the Netherlands. Emerging infectious diseases, 2017. 23(12): P. 2050-2054.
32. OIE, Update on highly pathogenic avian influenza in animals (type H5 and H7) [cited 2017 Mar 21]. http://www.oie.int/animal-health-in-the-world/update-on-avian-influenza/2017/. 2017.
33. Swayne, D.E., et al., Acute renal failure as the cause of death in chickens following intravenous inoculation with avian influenza virus A/chicken/Alabama/7395/75 (H4N8). Avian Dis, 1994. 38(1): P. 151-7.
34. Song, B.-M., et al., Pathogenicity of H5N8 virus in chickens from Korea in 2014. Journal of veterinary science, 2015. 16(2): P. 237-240.
35. Tanikawa, T., et al., Pathogenicity of H5N8 highly pathogenic avian influenza viruses isolated from a wild bird fecal specimen and a chicken in Japan in 2014. Microbiology and Immunology, 2016. 60(4): P. 243-252.
36. Anis A, AboElkhair M, Ibrahim M (2017) Characterization of highly pathogenic avian influenza H5N8 virus from Egyptian domestic waterfowl in 2017AVIAN PATHOLOGY https://doi.org/10.1080/03079457.2018.1470606.
37. Kandeil, A., Hicks, J. T., Young, S. G., El Taweel, A. N., Kayed, A. S., Moatasim, Y., Kutkat, O., Bagato, O., McKenzie, P. P., Cai, Z., Badra, R., Kutkat, M., Bahl, J., Webby, R. J., Kayali, G., & Ali, M. A. (2019). Active surveillance and genetic evolution of avian influenza viruses in Egypt, 2016-2018. Emerging microbes & infections, 8(1), 1370–1382.

38. Kareem E. Hassan, Noha Saad, Hassanein H. Abozeid, Salama Shany, Magdy F. El-Kady, Abdelsatar Arafa, Azza A.A. EL-Sawah, Florian Pfaff, Hafez M. Hafez, Martin Beer, Timm Harder,Genotyping and reassortment analysis of highly pathogenic avian influenza viruses H5N8 and H5N2 from Egypt reveals successive annual replacement of genotypes, Infection, Genetics and Evolution, 2020. 84,1567-1348..
39. Teijaro, J.R.; Walsh, K.B.; Cahalan, S.; Fremgen, D.M.; Roberts, E.; Scott, F. et al.(2011): Endothelial cells are central orchestrators of cytokine amplification during influenza virus infection. *Cell; 146: 980–991.*
40. Suzuki, K., et al., Association of increased pathogenicity of Asian H5N1 highly pathogenic avian influenza viruses in chickens with highly efficient viral replication accompanied by early destruction of innate immune responses. J Virol, 2009. 83(15): P. 7475-86.
41. Karpala, A.J., et al., Highly pathogenic (H5N1) avian influenza induces an inflammatory T helper type 1 cytokine response in the chicken. J Interferon Cytokine Res, 2011. 31(4): P. 393-400.
42. Vigeveno, R.M., et al., Outbreak Severity of Highly Pathogenic Avian Influenza A(H5N8) Viruses Is Inversely Correlated to Polymerase Complex Activity and Interferon Induction. J Virol, 2020. 94(11).

Table 1

Table.1 Viral titer of the three Egyptian H5N8 avian influenza viruses in swabs and different organs of infected and infected contact chickens

		S75	CA258	S/S19	F446	P value
SWABS Log10 (EID50)	2nd	3.7±1.4	3.47±1.26	2.3±1.01	6.02±1.03 *#$	< 0.001
	4th	6.49±0.62	4.25±1.57 *	4.19±1.2 *	7.6±1.52 #$	< 0.001
LUNG Log10 (EID50)	2nd	4.49±1.15	3.94±1.13	3.32±1.28	7.54±1.5 #$	0.016
	4th	5.72±0.74	5.14±0.04	3.67±1.44	8.71±0.25 *#$	< 0.001
Brain Log10 (EID50)	2nd	4.51±0.96	3.89±1.79	3.78±1.44	7.67±0.27 #$	0.016
	4th	4.53±0.75	5.65±0.49	1.7±0.07 *#	8.06±0.22 *#$	< 0.001
spleen Log10 (EID50)	2nd	5.32±0.66	3.23±1.28 *	4.22±0.56	7.92±0.02 *#$	< 0.001
	4th	5.2±0.03	2.95±0.29 *	2.1±0.17 *#	7.82±0.07 *#$	< 0.001
contact swab Log10 (EID50)	2nd	3.61±0.1		2.06±0.08 *	5.81±0.53 *$	0.003
	4th	3.58±1.66	1.69±0.09	1.68±0.45	5.52±0.08 #$	0.029

Values are presented as mean ±SD

*: statistically significant compared to corresponding value in S75 (P<0.05)

#: statistically significant compared to corresponding value in CA258 (P<0.05)

$: statistically significant compared to corresponding value in S/S19 (P<0.05)

Figures

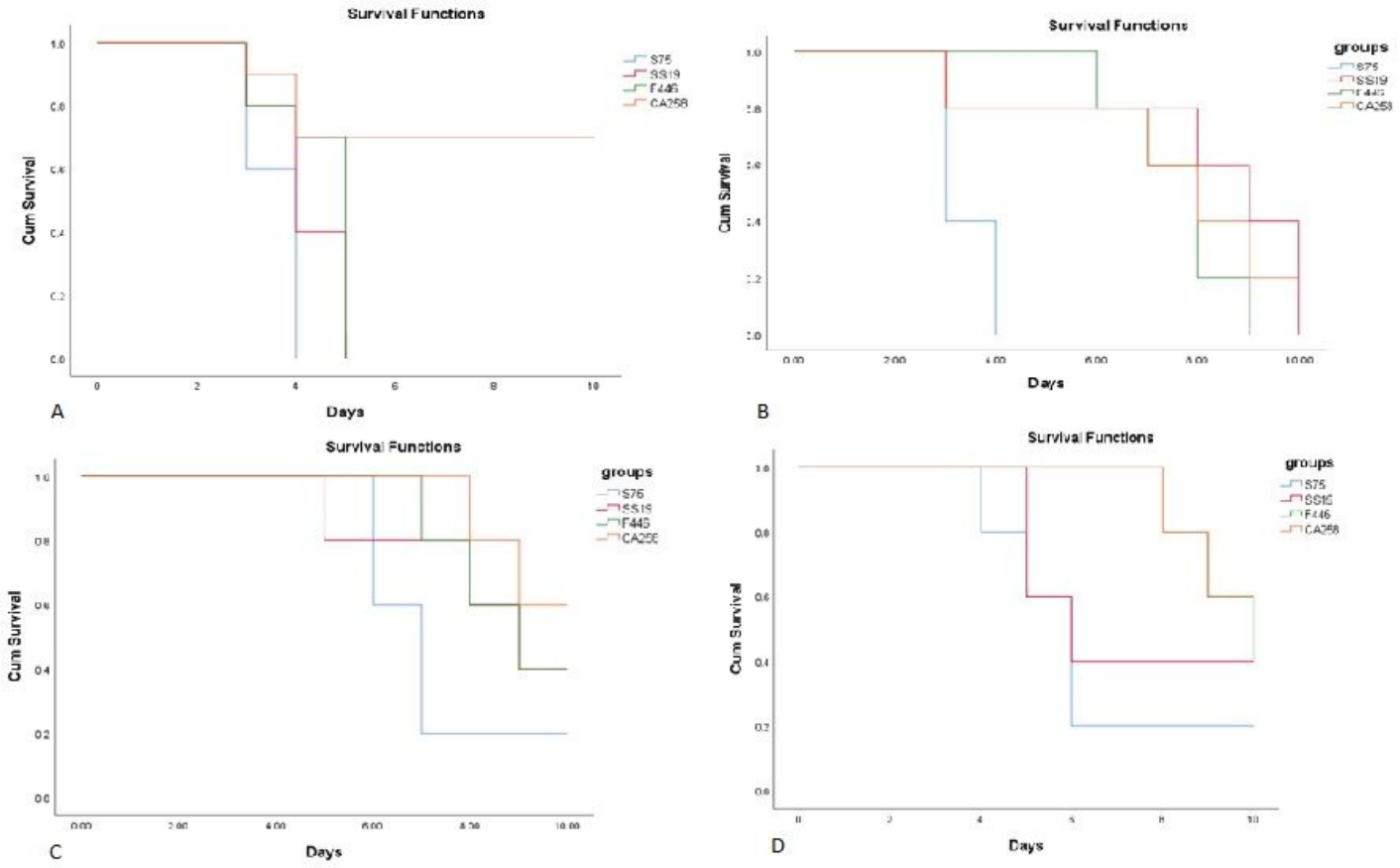

Figure 1

The survival rate of chickens inoculated intranasal with 106 (A), 105(B), 104 (C), and 103(D) egg infective dose of HPAI- CAO285, F446, SS19, and S75 represented by a closed diamond, closed square, closed triangle, and cross, respectively.

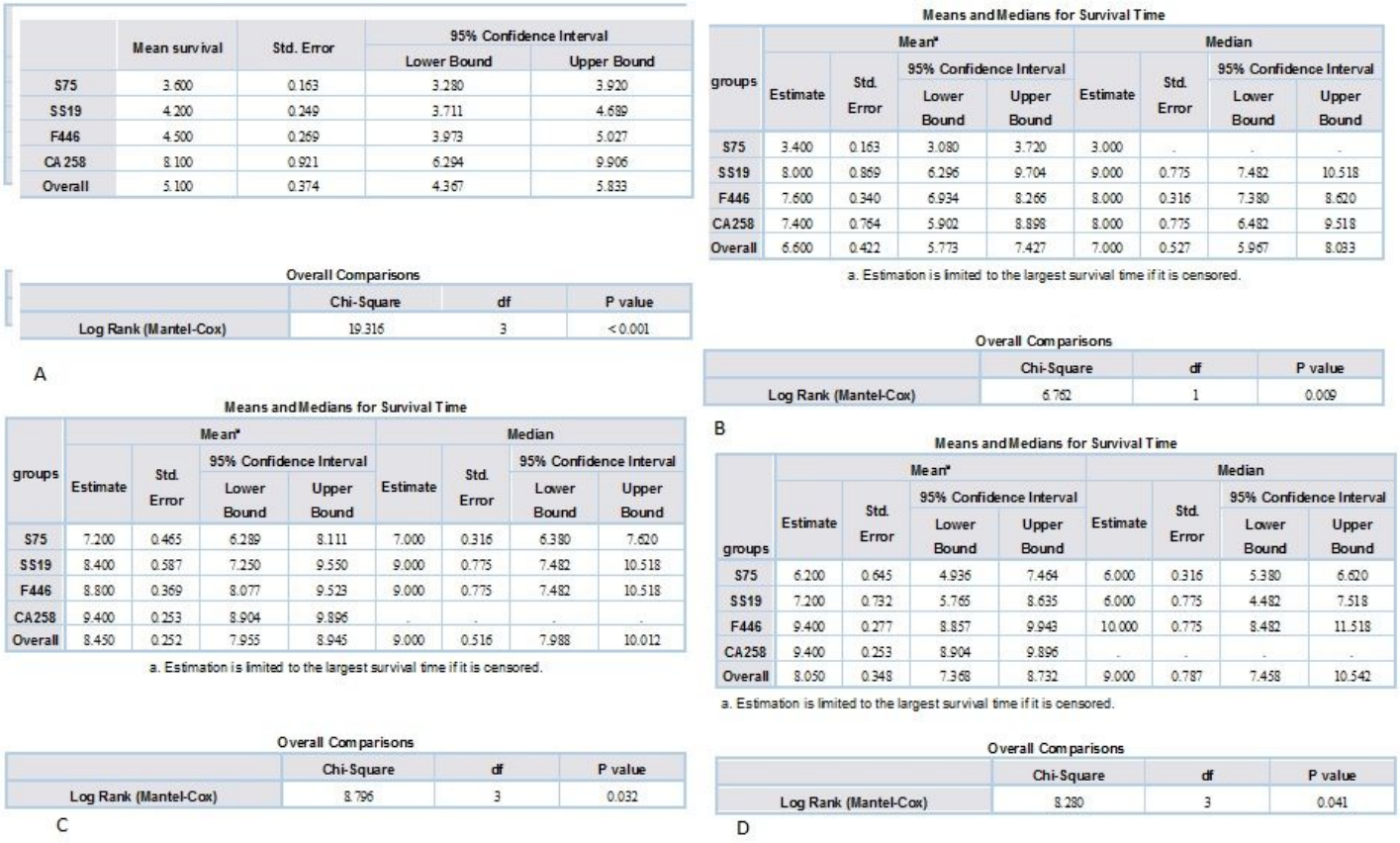

	Mean survival	Std. Error	95% Confidence Interval	
			Lower Bound	Upper Bound
S75	3.600	0.163	3.280	3.920
SS19	4.200	0.249	3.711	4.689
F446	4.500	0.269	3.973	5.027
CA258	8.100	0.921	6.294	9.906
Overall	5.100	0.374	4.367	5.833

Overall Comparisons

	Chi-Square	df	P value
Log Rank (Mantel-Cox)	19.316	3	< 0.001

A

Means and Medians for Survival Time

groups	Mean*				Median			
	Estimate	Std. Error	95% Confidence Interval		Estimate	Std. Error	95% Confidence Interval	
			Lower Bound	Upper Bound			Lower Bound	Upper Bound
S75	7.200	0.465	6.289	8.111	7.000	0.316	6.380	7.620
SS19	8.400	0.587	7.250	9.550	9.000	0.775	7.482	10.518
F446	8.800	0.369	8.077	9.523	9.000	0.775	7.482	10.518
CA258	9.400	0.253	8.904	9.896	.	.	.	.
Overall	8.450	0.252	7.955	8.945	9.000	0.516	7.988	10.012

a. Estimation is limited to the largest survival time if it is censored.

Overall Comparisons

	Chi-Square	df	P value
Log Rank (Mantel-Cox)	8.796	3	0.032

C

Means and Medians for Survival Time

groups	Mean*				Median			
	Estimate	Std. Error	95% Confidence Interval		Estimate	Std. Error	95% Confidence Interval	
			Lower Bound	Upper Bound			Lower Bound	Upper Bound
S75	3.400	0.163	3.080	3.720	3.000	.	.	.
SS19	8.000	0.869	6.296	9.704	9.000	0.775	7.482	10.518
F446	7.600	0.340	6.934	8.266	8.000	0.316	7.380	8.620
CA258	7.400	0.764	5.902	8.898	8.000	0.775	6.482	9.518
Overall	6.600	0.422	5.773	7.427	7.000	0.527	5.967	8.033

a. Estimation is limited to the largest survival time if it is censored.

Overall Comparisons

	Chi-Square	df	P value
Log Rank (Mantel-Cox)	6.762	1	0.009

B

Means and Medians for Survival Time

groups	Mean*				Median			
	Estimate	Std. Error	95% Confidence Interval		Estimate	Std. Error	95% Confidence Interval	
			Lower Bound	Upper Bound			Lower Bound	Upper Bound
S75	6.200	0.645	4.936	7.464	6.000	0.316	5.380	6.620
SS19	7.200	0.732	5.765	8.635	6.000	0.775	4.482	7.518
F446	9.400	0.277	8.857	9.943	10.000	0.775	8.482	11.518
CA258	9.400	0.253	8.904	9.896	.	.	.	.
Overall	8.050	0.348	7.368	8.732	9.000	0.787	7.458	10.542

a. Estimation is limited to the largest survival time if it is censored.

Overall Comparisons

	Chi-Square	df	P value
Log Rank (Mantel-Cox)	8.280	3	0.041

D

Figure 2

A Kaplan-Meier survival curve with calculation of median survival and unpaired log rank test for significant differences in the survival between the HPAI- CAO285, F446, SS19, and S75 with 106 (A), 105(B), 104 (C), and 103(D) egg infective dose.

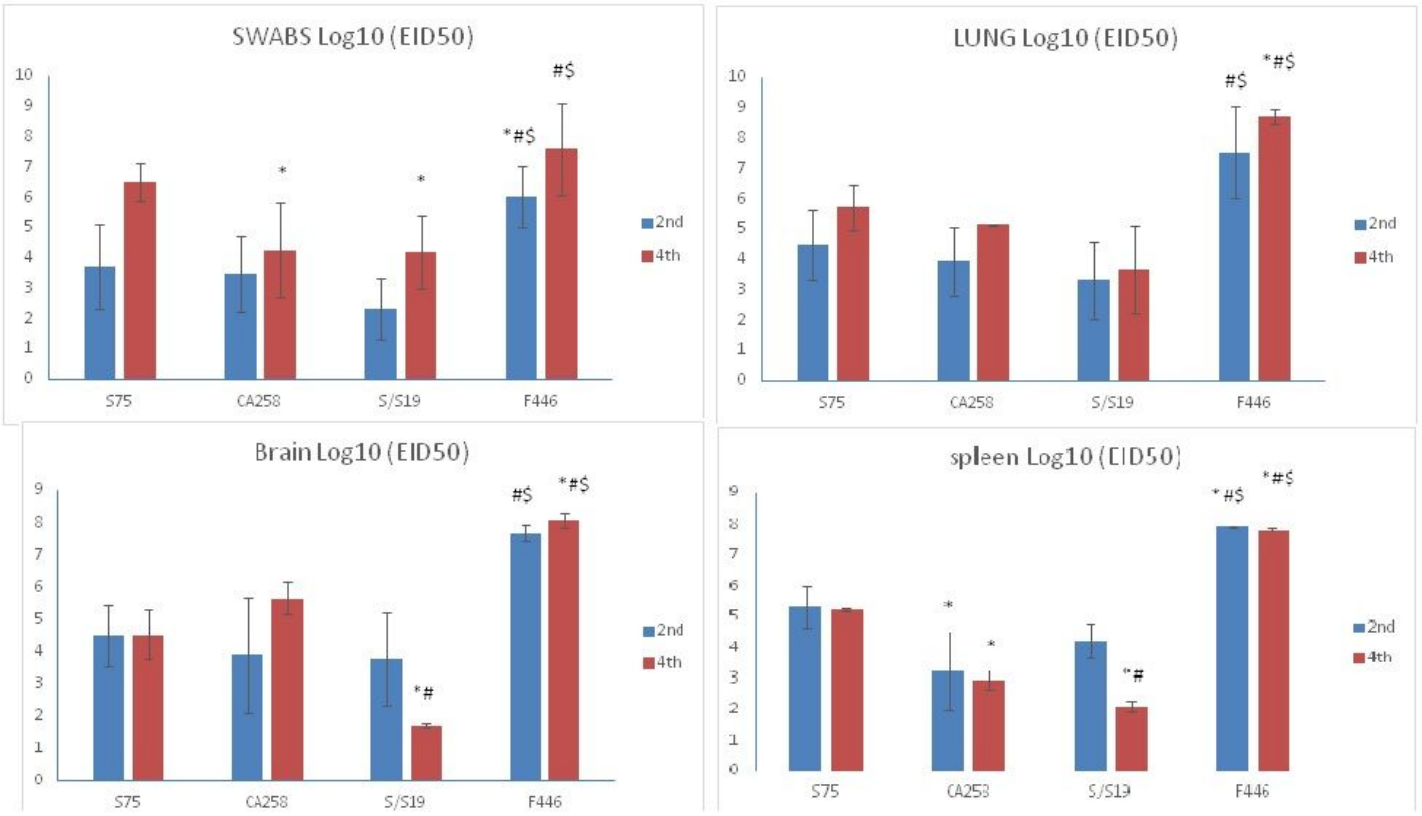

Figure 3

Viral titers in swabs, lung, brain, and spleen tissues of infected chickens at 2 and 4 dpi with S75, CAO285, SS19, and F446. *: statistically significant compared to corresponding value in S75 (P<0.05), #: statistically significant compared to corresponding value in CA258 (P<0.05) and $: statistically significant compared to corresponding value in S/S19 (P<0.05)

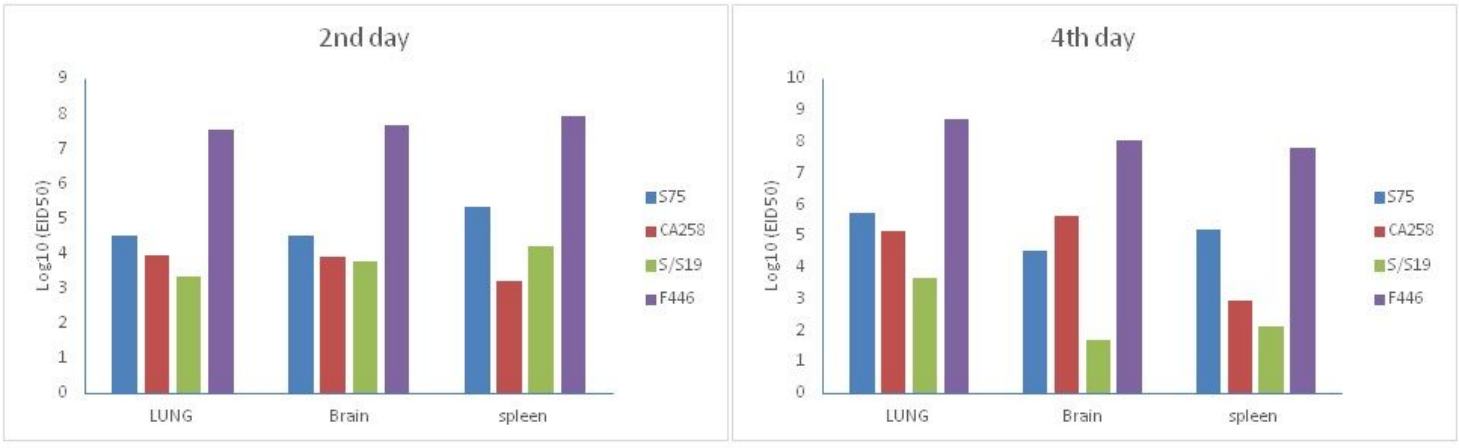

Figure 4

viral titer in lung, brain spleen tissue of infected chicken at 2 and 4 dpi with S75, CAO285, SS19, and F446.

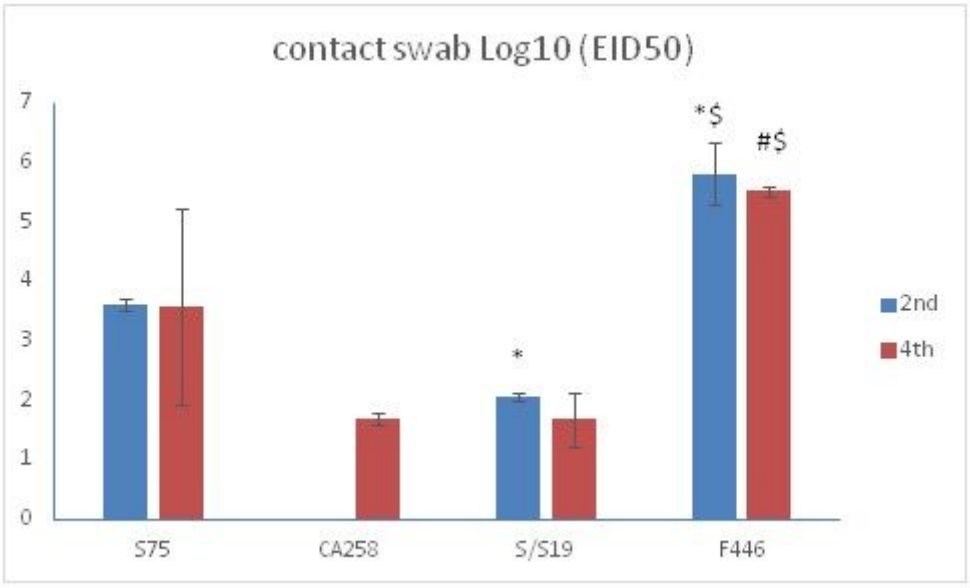

Figure 5

Viral titers in swabs of infected contact chickens at 2 and 4 dpi with S75, CAO285, SS19, and F446. *:statistically significant compared to corresponding value in S75 (P<0.05), #: statistically significant compared to corresponding value in CA258 (P<0.05) and $: statistically significant compared to corresponding value in S/S19 (P<0.05)

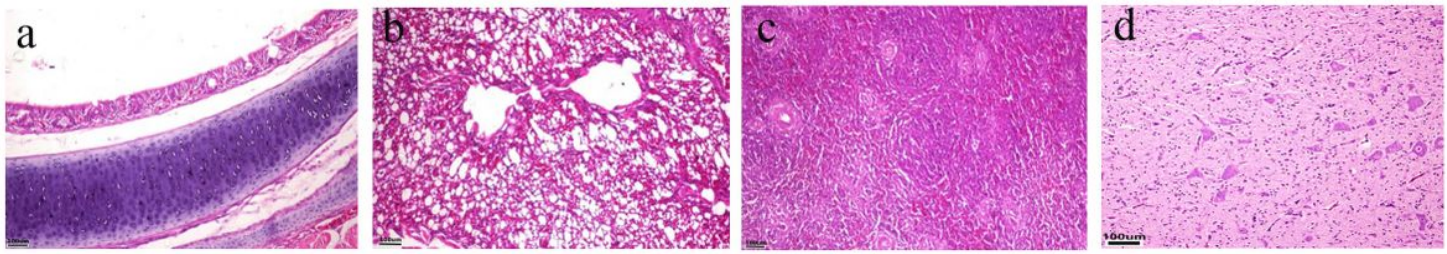

Figure 6

showed normal histological picture of trachea, lung, spleen and brain sequentially of negative control group.

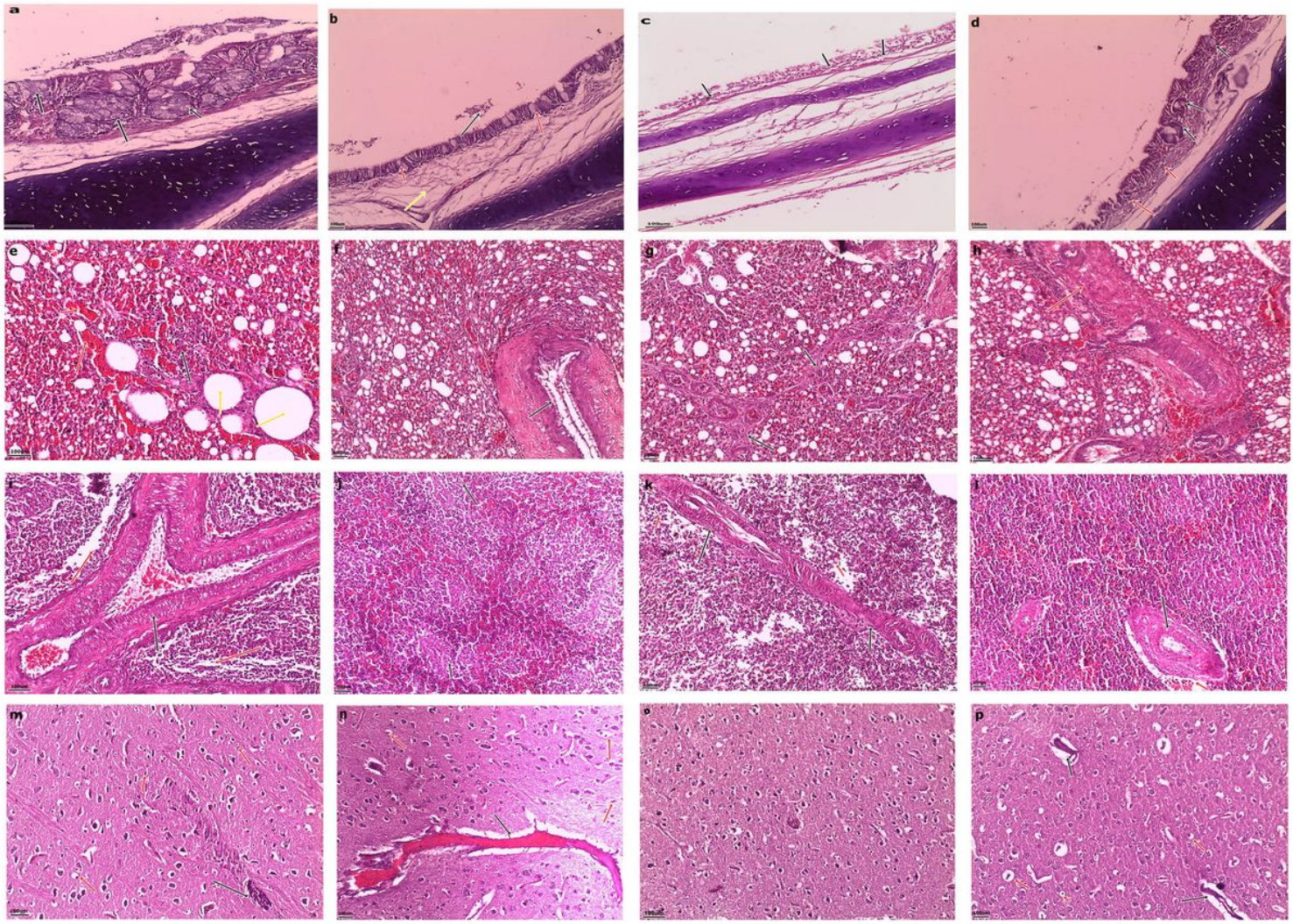

Figure 7

organs of chickens 2 dpc infected H5N8 and H5N1. (a) trachea of F446 showing submucosal edema (black arrow) and congested blood vessels (red arrow), (b) trachea of SS19 submucosal hemorrhages (arrow), (c) trachea of CA258 showing activation of mucous gland (yellow arrow) with severe submucosal edema (black arrow)and inflammatory cells infiltration (red arrow), (d) trachea of S75 showing necrosed mucosal layer (arrow). (e) lung of F446 showing intraluminal exudate (black arrow) with necrosed 3ry bronchi epithelium (yellow arrow), (f) lung of SS19 showing thickening blood vessel (arrow), (g) lung of CA258 showing thrombus formation (black arrow) with perivascular lymphocytic cells (red arrow), (h) lung of S75 showing congested blood vessels (red arrow) with lymphocytic cells infiltration (black arrow), (i & j) spleen of F446 & SS19 showing arteriosclerosis (black arrow) and necrosis (red arrow), (k & l) spleen of CA258 & S75 showing normal picture, (m) brain of F446 showing hemorrhages (arrow), (n & p) brain of SS19 showing congested blood vessels (red arrow) and neuronal necrosis (black arrow), (o) brain of CA258 showing gliosis. (Scale bare = 100um)

Figure 8

(figure 8 is not included with this submission) Figure (8): organs of chickens 4 dpc infected H5N8 and H5N1. (a) trachea of F446 showing hyperplasia of goblet cells (arrow) (b) trachea of SS19 activation of mucous gland (red arrow) submucosal edema (yellow arrow) with lymohocytic cells infiltration (black arrow), (c) trachea of CA258 showing necrosed mucosal layer (black arrow), (d) trachea of S75 activation of mucous gland (black arrow) with lymphocytic cells infiltration (red arrow). (e) lung of F446 showing lymphocytic cells infiltration (black arrow) with compensatory alveoli formation (yellow arrow) and hemorrhages (red arrow), (f) lung of SS19 showing vasculitis (arrow), (g) lung of CA258 showing pulmonary necrosis (arrow), (h) lung of S75 showing severe vasculitis (arrow), (i) spleen of F446 showing arteriosclerosis (black arrow) and lymphocytic deplestion (red arrow), (j) spleen of SS19 showing necrosis (arrow), (k & l) spleen of CA258 & S75 showing vasculitis (black arrow) with heterophilic infiltration (red arrow), (m) brain of F446 showing neuronal necrosis (red arrow) with perivascular cuffing (black arrow), (n & p) brain of SS19 showing congested blood vessels (black arrow) and neuronal necrosis (red arrow), (o) brain of CA258 showing cerebral edema and gliosis 2dpi (fig. 7o) which increased 4dpi (fig. 8o). (Scale bare = 100um)